1   **Brain enlargement and dental reduction were not linked in hominin evolution**

2

3   Aida Gómez-Robles[a,1], Jeroen B. Smaers[b], Ralph L. Holloway[c], P. David Polly[d],

4   Bernard Wood[a]

5

6   [a] Center for the Advanced Study of Human Paleobiology, Department of Anthropology,

7   The George Washington University, Washington, DC 20052, USA.

8   [b] Department of Anthropology, Stony Brook University, Stony Brook, NY 11794, USA.

9   [c] Department of Anthropology, Columbia University, New York, NY 10027, USA.

10   [d] Department of Geological Sciences, Indiana University, Bloomington, IN 47405,

11   USA.

12

13   [1] To whom correspondence should be addressed. Email: agomezrobles@gwu.edu

14

15   **Abstract**

16   The large brain and small postcanine teeth of modern humans are among our most

17   distinctive features, and trends in their evolution are well studied within the hominin

18   clade. Classic accounts hypothesize that larger brains and smaller teeth co-evolved

19   because behavioral changes associated with increased brain size allowed for a

20   subsequent dental reduction. However, recent studies have found mismatches between

21   trends in brain enlargement and posterior tooth size reduction in some hominin species.

22   We use a multiple variance Brownian motion approach in association with evolutionary

23   simulations to measure the tempo and mode of the evolution of endocranial and dental

24   size and shape within the hominin clade. We show that hominin postcanine teeth have

25   evolved at a relatively consistent neutral rate, whereas brain size evolved at

26   comparatively more heterogeneous rates that cannot be explained by a neutral model,

27   with rapid pulses in the branches leading to later *Homo* species. Brain reorganization

28   only shows evidence of elevated rates much later in hominin evolution, suggesting that

29   fast-evolving traits, such as the acquisition of a globular shape, may be the result of

30   direct or indirect selection for functional or structural traits typical of modern humans.

31

32   **Keywords**

33   Endocast, postcanine teeth, evolutionary rates, selection, paleoanthropology

34

35   **Significance statement**

36   The evolution of posterior teeth and brains seems to follow parallel trends in hominins.

37   Larger brain size is associated with reduced premolar and molar crowns, but this

38   association is not observed in all hominin species. We have evaluated this association in

39   a quantitative way by measuring lineage-specific rates of dental and cerebral evolution

40   in the different branches of the hominin evolutionary tree. Our results show that

41   different species evolved at different rates, and that brain evolution in early *Homo* was

42   faster than dental evolution. This result points to different ecological and behavioral

43   factors influencing the evolution of hominin teeth and brains.

44

45   /body

46

47   **Introduction**

48

49   The large brains and small posterior teeth of modern humans are among our most

50   distinctive features, and trends in their evolution are well studied because of the

2

phylogenetic and functional implications of variation in dental and cerebral anatomy (1-3). Brain expansion and postcanine reduction appear to follow parallel trends during hominin evolution and classic views consider that an increase in brain size was linked to a more complex behavior that included the manufacture and use of stone tools, which allowed for a subsequent dental reduction. A shift towards a higher-quality diet during the evolution of early *Homo* has also been related to brain size increase and posterior tooth reduction (4, 5). However, it has recently been suggested that in early *Homo* brain expansion —as inferred from endocranial capacity— substantially preceded dental reduction (6). It has also been noted that early in the Neanderthal lineage dental reduction preceded the additional brain expansion seen in the later 'classic' Neanderthals (7). The suggestion that stone tool use and manufacture substantially predated the increase in brain size observed in early *Homo* (8) adds further complexity to this scenario.

Recent developments in ancestral state reconstruction (9, 10) allow lineage-specific patterns of brain expansion and dental reduction to be quantified and compared. Unlike traditional approaches to ancestral state reconstruction that assume a neutral evolutionary scenario, which is likely unrealistic in most cases, we used a variable rate approach that estimates differences in evolutionary rates across different branches of a given phylogeny. We applied this approach to quantitative data on endocranial and postcanine dental size and shape in order to develop a comprehensive scenario of trends in endocranial and dental evolution across the hominin clade (Fig. 1). Our assessment used a framework phylogeny based on widely agreed evolutionary relationships and on the currently estimated first and last appearance dates for eight of the most broadly accepted hominin species (11) (Fig. 1, Table S1). Amounts of change along each branch

76   of the hominin phylogenetic tree estimated through the variable rate approach were

77   compared with the amount of change observed in evolutionary simulations that used a

78   constant variance Brownian motion (BM) model (12) in which traits evolve neutrally

79   and at a constant rate, without directional trends in any particular branch of the hominin

80   phylogeny (Methods).

81

82   **Results**

83   Among the four traits, endocranial volume is the only one whose evolution has given

84   rise to patterns of variation that are significantly different from those obtained from

85   neutral simulations (Fig. S1). The standard deviation of the amounts of change per

86   branch observed across the phylogeny is significantly greater than the standard

87   deviations obtained in constant-rate simulations of the evolution of endocranial size

88   ($P=0.017$). This indicates that lineage-specific patterns of brain size evolution are more

89   heterogeneous than expected under a neutral model and unlikely to be explained by

90   genetic drift. In addition, the rates of change for endocranial and dental size and shape

91   through time differ substantially in different parts of the hominin phylogeny (Figs. 2

92   and 3). These differences are robust to different sample composition ($P<0.001$ for all the

93   pairwise comparisons between the four traits) and to corrections for small sample size

94   (Fig. S2), and they are substantial for most branches of the hominin phylogeny (Table

95   S2, Fig. S3). Although we use the term *rate* to make reference to branch-specific

96   amounts of change, it should be noted that these values are not rates in the strict sense

97   because they do not represent amounts of change per unit of time, but the ratio of

98   observed to simulated change per branch (see Methods).

99

100 Our results show that sustained rapid evolution in brain size started before the

101 separation of *Paranthropus* and *Homo,* and peaked before the divergence between *H.*

102 *erectus* and the lineage leading to Neanderthals and modern humans (Fig. 3A). That

103 peak rate was more than 4 times greater than that observed in simulated neutral

104 scenarios (Table S2). Additional rapid brain increase was observed in the lineage

105 immediately predating the Neanderthal-modern human split, but this was only twice as

106 fast as that observed in a neutral scenario (Table S2). Other branches within the hominin

107 phylogeny show much slower rates of change than those observed in a pure BM

108 process, which is consistent with stabilizing selection and constrained evolution. These

109 estimates are similar to the ones obtained when using a more traditional approach to

110 quantify branch-specific change based on a generalized least squares (GLS) ancestral

111 reconstruction method (Table S3), which detects fast and slow evolutionary rates in the

112 same branches, but with less extreme values.

113

114 Our results support the long-standing hypothesis that within the hominin clade brain

115 organization, as inferred from endocranial shape, evolved independently of brain size

116 (13). The ratios between the endocranial shape change measured along each branch and

117 those simulated using BM were all close to 1, leading to a general scenario that is not

118 statistically different from those observed in constant-rate simulations (P=0.355, Fig.

119 S1). This indicates that endocranial shape evolved according to a quasi-neutral model,

120 which is consistent with a scenario where genetic drift is predominant (Fig. 3B). Rapid

121 change, about twice that expected under a BM model, was observed only along the

122 branch leading to modern humans from their last common ancestor with Neanderthals

123 (Table S2). This rapid evolutionary change is reflected in the principal component

124 analysis of endocranial shape variation, which shows that *H. sapiens* strongly diverges

125   from all other species along PC1 (Fig. 2B). The eigenvector of this axis shows that the

126   dorsal arc connecting the frontal and occipital poles is the only variable loading

127   positively on PC1, thus separating flatter from the more globular endocasts that

128   distinguish *H. sapiens* (14-16) (Table S4). Researchers have suggested that

129   globularization is driven by upper parietal reorganization, and that this anatomical

130   change can be associated with enhanced visuospatial integration and memory in modern

131   humans (17). The comparatively fast evolution of the dorsal arc trait in the lineage

132   leading to *H. sapiens* is consistent with such a link between brain anatomy and function,

133   although it could be an indirect result of selection on other craniofacial hard-tissue

134   changes (18). If some individuals that do not show a globular anatomy, such as Jebel

135   Irhoud 1 and 2, and Omo 2, are early members of *H. sapiens* (19), then the endocranial

136   anatomy typical of modern humans may have evolved within the *H. sapiens* lineage.

137

138   Although there are differences in branch-specific evolutionary rates for dental size, they

139   are still within the expectations of a constant-rate model (P=0.257, Fig. S1). Sustained

140   reduction in the posterior dentition began in the branches antedating the origin of the

141   genus *Homo* and continued along the sequence of branches leading to *H. sapiens* (Figs.

142   2C and 3C). Dental reduction along all these branches occurred at a rate that was

143   approximately twice as fast as expected under a neutral evolutionary model (Table S2).

144   Although the size of posterior teeth of *H. habilis* and *A. afarensis* is similar, a fast

145   evolutionary rate is inferred before the evolution of early *Homo* because this change is

146   calculated with respect to the last common ancestor of *Paranthropus* and *Homo*, which

147   is inferred to have had larger posterior teeth than *A. afarensis* (Fig. 2C). A rapid rate of

148   dental reduction continued on the lineage leading to modern humans, but not in

149   Neanderthals, resulting in the comparatively small postcanine dentition of our species

6

150 [Fig. 2C, ref. (20)]. A previous quantitative study of molar size found that molar

151 reduction observed in *H. erectus*, Neanderthals and modern humans occurred at a faster

152 rate than in early *Homo* (21). That study, however, used M2 area as a proxy for molar

153 size without considering variation in molar proportions across the molar row. Those

154 proportions are known to change in the genus *Homo* in concert with absolute molar size,

155 thus making M2s and M3s disproportionately small in species with overall small dental

156 size (22, 23). Reduction in the dentition was not the only rapidly evolving trend because

157 dental expansion occurred at similarly high rates in the lineage leading to *Paranthropus*

158 species (Fig. 2C, Table S2). Our data suggest that posterior tooth size in *P. robustus*

159 stabilized after its divergence from the *P. boisei* lineage, whereas *P. boisei* continued its

160 dental expansion, but in a way consistent with quasi-neutral evolution. Assuming that

161 the *Paranthropus* clade is monophyletic, which is the most common assumption even if

162 other explanations are possible (24), these observations suggest that *Paranthropus*

163 postcanine megadontia is the result of long term selective pressures that predate the

164 divergence of the *Paranthropus* species.

165

166 As with endocranial shape, the shape of tooth crowns also evolved under a quasi-neutral

167 model in which the evolutionary change along each branch is close to and statistically

168 indistinguishable from that expected from a pure BM model (P=0.528, Fig. 3D, Fig.

169 S1). The difference that drives the first principal component of dental crown shape is a

170 preferential reduction of the distal areas of premolars and molars in Neanderthals and

171 modern humans (Fig. 2D; Fig. S4). The most rapid evolutionary change on the tree (1.5

172 times greater than that expected in a neutral scenario) is associated with this change

173 along the branch antedating the separation of Neanderthals and modern humans (Table

174 S2). Although both species share strong reduction of the distal regions of posterior

7

175 teeth, they have their own species-specific configurations. The characteristically derived

176 dentition of Neanderthals (25, 26) is reflected in the relatively fast rate of evolution of

177 dental shape in this lineage (Table S2).

178

179 **Discussion**

180 Our results show clear differences in evolutionary patterns corresponding to endocranial

181 and dental size and shape during hominin evolution. Endocranial volume evolved at

182 relatively heterogeneous rates that differ significantly from those observed under a

183 constant-rate neutral model (Fig. S1). Endocranial shape and dental size and shape

184 evolved at comparatively more uniform rates, with shape traits evolving under a quasi-

185 neutral model. Although the evolution of these traits does not significantly differ from

186 the expectations of a constant-rate scenario, endocranial shape, dental size and dental

187 shape still show significantly different evolutionary patterns. Given similar genetic

188 variance, drift is expected to affect all traits in the same population equally (27). Studies

189 of brain anatomy in chimpanzees and modern humans, however, have shown that brain

190 size and brain organization have substantially different heritabilities (28), which

191 represent the proportion of total phenotypic variance in a population that has a genetic

192 basis. Therefore, genetic variances of the traits included in our study can plausibly be

193 different, which might explain their different evolutionary behavior even if neither

194 significantly differs from neutrality.

195

196 The observed patterns of branch-specific variation are consistent regardless of sample

197 size and composition (Fig. S2), but they could be affected by changes in the

198 phylogenetic scenario. We have chosen to deal with phylogenetic uncertainty by

199 removing from our analyses those species whose phylogenetic position is particularly

200   controversial, such as *H. ergaster, H. antecessor* and *H. heidelbergensis*. The resulting

201   phylogenetic topology generally agrees with most quantitative and qualitative

202   assessment of hominin phylogenetic relationships (21, 29, 30), but new fossil findings

203   resulting in different relationships or branch lengths could potentially modify some of

204   our findings.

205

206   Our results, which indicate that the evolution of hominin brain organization and brain

207   size are decoupled, are consistent with larger brain size being positively selected across

208   the entire genus *Homo* (31). Strong selection for larger brains has been linked to the

209   selective advantages associated with the enhanced computational abilities of a larger

210   neocortex with more neurons (32), but it can be also linked to other neural

211   modifications such as an increased developmental plasticity arising from changes in the

212   developmental patterns associated with larger brains (28, 33, 34). Selection for certain

213   aspects of brain organization, particularly in the upper parietal reorganization that is

214   arguably associated with modern human-specific functional modifications (17), is

215   confined primarily to the branch leading directly to *H. sapiens.* No other aspects of

216   brain reorganization as described by our set of variables show evidence of fast evolution

217   across the hominin clade. However, many aspects of brain reorganization are not

218   captured by those endocranial metrics, particularly those related to finer-grained

219   organization such as sulcal variation and brain asymmetries, among others. The

220   predominant role of neutral mechanisms in the evolution of endocranial shape is

221   consistent with previously published work reporting a major role of genetic drift in

222   craniofacial evolution during the *Australopithecus-Homo* transition (35, 36) and during

223   the divergence of Neanderthals and modern humans (37). Although our study focuses

on endocranial variation, our findings are consistent with a general neutral scenario for the evolution of craniofacial shape in hominins.

The evolution of tooth crown size and shape are more closely linked than are the evolution of brain size and shape. The branch antedating the separation of Neanderthals and modern humans is characterized by strong reduction in overall dental size associated with strong localized reduction of the distal area of the crown of all postcanine teeth (20, 26). This anatomical change, however, took place over a long period of time and does not show evidence of particularly fast evolution indicating strong selection. Although *H. sapiens* shows substantially faster reduction in dental size than Neanderthals, the two species share similar evolutionary rates of crown shape evolution, thus demonstrating that their species-specific dental traits have been subject to similar selection intensities. Crown shape evolution does not radically depart from a Brownian motion model and most branches within the hominin phylogeny have evolved at very similar rates with respect to postcanine dental shape. This observation lends quantitative support to dental shape as a useful proxy for reconstructing phylogenetic relationships in hominin fossil species. Indeed, the utility of dental shape to infer evolutionary relationships is also supported by recent DNA analyses of Middle Pleistocene European fossils (38, 39), which have confirmed their relationship with Neanderthals, as it was initially proposed using fossil evidence (7, 26).

If branch-specific trends are not quantified, the sustained brain expansion found in some of the branches of the genus *Homo* may appear to be associated with sustained dental reduction. However, our results, which show that teeth and brains evolved at different rates in different hominin species, suggest that the two trends were "decoupled". Our

249   analysis shows that the apparent coupling of the traits is confined to the three branches

250   that connect the last common ancestor of *Paranthropus* and *Homo* with the last

251   common ancestor of Neanderthals and modern humans and that, even in those cases,

252   brain evolution occurred at faster rates. We suggest that the context-specific ecological

253   and behavioral factors that influenced the evolution of teeth and brains were not the

254   same for the two morphological regions, nor were the combinations of those factors the

255   same at different stages during hominin evolution.

256

257   **Materials and methods**

258   **Materials** We used four datasets to evaluate postcanine and endocranial size and shape

259   (Table S1, Datasets 1-4). The dental size and shape dataset was assembled by one of us

260   (AGR) as part of quantitative descriptions of occlusal postcanine morphology (26, 40).

261   Those samples were pruned to include only species with relatively uncontroversial

262   phylogenetic positions (see below), and for which data on endocranial size and shape

263   were also available. Endocranial size was studied using species-specific endocranial

264   volumes based on values listed in ref. (41). This data set does not reflect the reduction

265   in endocranial volume seen in recent *Homo sapiens*. Mean cranial capacity in *Homo*

266   *erectus* was estimated from a subsample of Asian *Homo erectus* that shares a similar

267   geographical and chronological origin as the dental sample (41). Endocranial shape was

268   evaluated in a smaller sample of complete or partial hominin endocasts.

269

270   **Quantitative description of dental and endocranial size and shape** Postcanine dental

271   shape was characterized with configurations of landmarks and sliding semilandmarks

272   on the occlusal surface of tooth crowns (26, 40) and dental size was quantified as the

273   centroid size of those configurations (defined as the square root of the sum of the

11

274 squared distances between each landmark and the center of gravity of the

275 configuration). Procrustes superimposition (42) was used to remove variation in

276 position, size, and orientation, and species-specific mean shapes were obtained by

277 averaging Procrustes-superimposed coordinates for each species (26). Principal

278 components analyses of Procrustes coordinates were used to obtain the principal

279 component (PC) scores used in subsequent analyses (12). When all dimensions of shape

280 variation are considered, which we did throughout all our analyses, PC scores contain

281 the same information as original variables, but they are mathematically more convenient

282 (12).

283

284 The size and shape data were pooled to analyze the complete postcanine dentition. For

285 shape analyses, landmark coordinates corresponding to the ten postcanine teeth (upper

286 and lower premolars and molars) were subjected to different Procrustes

287 superimpositions, and were then combined in the same principal components analyses.

288 Overall dental size was estimated by summing up centroid sizes across all the

289 postcanine teeth. Analyses of dental size, therefore, reflect increases or decreases of

290 total postcanine occlusal areas, but not changes in dental proportions among teeth.

291

292 Endocranial size was evaluated using species-specific mean endocranial volumes.

293 Endocranial shape was quantified using a set of classic linear metrics measured by

294 RLH. These metrics included eight variables used in other studies of hominin

295 endocranial variation (Fig. 1, ref. 43). Size variation was removed from these analyses

296 by dividing each of these metrics by the cube root of cranial capacity in each individual.

297 Species-specific mean values for each of these variables were subjected to principal

298   components analysis, and PC scores were used in ancestral reconstructions of

299   endocranial shape.

300

301   The robustness of our results to sample composition was evaluated by bootstrapping the

302   original samples 1,000 times, and then recalculating species-specific mean values and

303   running all the analyses in bootstrapped samples. Likewise, we assessed if the more

304   heterogeneous evolutionary rates obtained for endocranial evolution with respect to

305   dental evolution result from differences in sample size. Because some of the species in

306   our samples are represented by only 3 endocasts, we jackknifed all the samples to three

307   individuals per species. This down-sampling process was also repeated 1,000 times.

308   Resampling rounds for both approaches were performed independently for each tooth

309   position because most individuals in the dental samples do not preserve all postcanine

310   teeth.

311

312   **Hominin phylogeny** Because our methodological approach requires the use of an *a*

313   *priori* phylogeny, we used only species whose phylogenetic positions are relatively

314   uncontroversial. Following the most widely accepted view, we considered *Homo* and

315   *Paranthropus* as two monophyletic clades (29) [but see ref. (44)]. *A. africanus* was

316   considered to be a sister group to both *Paranthropus* and *Homo* clades following ref.

317   (45), although some analyses have suggested other phylogenetic positions for this

318   species (29), including a recent classification as a sister group only to *Homo* (30). We

319   chose not to use a pruned version of the recently published Bayesian phylogeny

320   proposed in ref. (30) for two reasons. Firstly, the supermatrix on which this analysis is

321   based pools traits and character states based on different studies, criteria and scoring

322   systems, which may bias results by recovering nodes that have little or no support or by

13

323   failing to recover nodes that do have high support (46). Secondly, posterior probabilities

324   yielded by this analysis for most of the nodes included in our phylogeny are very low.

325   Although unquestionably valuable for considering alternative scenarios for hominin

326   evolution, we believe that evolutionary relationships reflected in the summary of best

327   trees presented in ref. (30) have in general weaker support than the relationships used in

328   our study.

329

330   Times of node divergence and ages of terminal species followed ref. (11). Tips were

331   dated to the last appearance date (LAD) for each species listed in Table 1 of ref. (11),

332   whereas nodes were dated to the corresponding first appearance date (FAD). Assuming

333   that FADs and LADs observed in the fossil record are unlikely to represent the actual

334   FADs and LADs for each species, we used the non-conservative version of these dates,

335   which incorporate "the age, and the published error of the age, of the nearest underlying

336   dated horizon in the case of the FAD, and the age, and the published error of the age, of

337   the nearest overlying dated horizon in the case of the LAD" [ref. (11), p. 55].

338

339   To account for some phylogenetic patterns that are not reflected in these values, we

340   dated the oldest ancestor in our tree to 4.4 Ma assuming an evolutionary continuity

341   between *A. anamensis* and *A. afarensis* (47), which was dated to 2.9 Ma. The

342   divergence between *P. robustus* and *P. boisei* was established at 2.3 Ma. To account for

343   the recent early *Homo* findings that have pushed back the FAD of the genus *Homo* to at

344   least 2.8 Ma (48), we set the origin of this genus at 2.9 Ma. The divergence of the

345   *Paranthropus* and *Homo* clades was estimated at 3.5 Ma. Because our samples do not

346   include late *H. erectus* fossils, we dated *H. erectus* to 400 ka. An early Neanderthal

347   status for Sima de los Huesos hominins is strongly supported by both the

348   paleontological and molecular evidence (7, 38, 49), so we established the divergence

349   date of Neanderthals and modern humans at 0.5 Ma, although morphological studies

350   suggest that an earlier divergence time for these species is likely (26, 30). The averaging

351   of data points at the last appearance dates used for each species is likely to provide

352   conservative estimates of branch-specific amounts of change. However, the use of data

353   at time points that are closer to individual values would artificially inflate the measured

354   amounts of change per branch due to the uncertainty regarding finer-grained population-

355   specific dates and their particular relationships.

356

357   **Ancestral estimation** A multiple variance Brownian motion (mvBM) framework was

358   used to estimate ancestral values in the hominin phylogeny (10). Most ancestral

359   estimation approaches assume a standard Brownian motion model of character

360   evolution (BM) (50). In standard BM the rate of evolution is assumed to have a single

361   mean and variance across all branches, and trait divergence is proportional to the square

362   root of time. Biologically, these assumptions imply there is no sustained difference in

363   the direction and rate of change among the different lineages of the phylogeny. In many

364   cases we expect this assumption to be unrealistic because selection may be associated

365   with environments that differ systematically between subclades or with particular

366   evolutionary or environmental events that occurred on only one branch of the tree, thus

367   producing different evolutionary rates and directions in different lineages. Our approach

368   relaxes the pure BM model in order to capture different patterns of trait variation along

369   each branch of the phylogeny (10).

370

371   Specifically, ancestral values were estimated using a two-step process. The first step

372   infers branch-specific patterns of change based on a model that assumes that trait values

15

373   for ancestral nodes are a compromise between global and local effects. The baseline

374   assumption that phylogenetic relatedness accurately reflects how traits evolve is hereby

375   leveraged against local deviations from this expectation. Specifically, a 'global'

376   estimate (a weighted estimate based on the phylogenetic tree and the tip values) is

377   combined with a 'local' estimate (accounting for information from a node's closest

378   relatives without taking tree structure into account) in order to accurately capture

379   lineage-specific changes that may deviate from the baseline expectation that

380   phylogenetic relatedness provides an accurate proxy of how traits evolve. Measures of

381   the rate of evolution are then estimated by dividing the squared trait difference by the

382   branch length for each ancestor-descendant pair. Rates hereby represent the extent to

383   which lineage-specific changes are found to align with the baseline expectation that

384   phylogenetic relatedness is an accurate proxy for trait evolution. Each branch rate can

385   be considered to be a point estimate of the rate of change along each individual branch

386   under a multiple variance BM model.

387

388   In the second step, the branch lengths of the original phylogenetic tree are rescaled

389   according to the estimated rates of evolution in order to account for branch-specific

390   differences from the baseline expectation that phylogenetic relatedness only is an

391   accurate proxy of trait evolution. The model with the rescaled branches is then

392   parameterized using a standard BM model in order to produce ancestral estimates. This

393   procedure makes use of the analytical power of BM estimation techniques while

394   allowing for local variation in evolutionary rates. This method —which is explained in

395   greater detail in ref. (10) and implemented in the R package 'evomap' (51)— was

396   applied to the hominin phylogeny and endocranial and dental datasets.

397

Evolutionary simulations Results obtained through the previously described process

were compared with results obtained through a simulated pure BM scenario. For size

traits, evolutionary variation was simulated on log-transformed size values, whereas for

shape variation, PC scores were used (12). Simulations were initiated at the ancestral-

most values estimated through the mvBM approach. A per-generation variance rate

(per-generation σ^2) was estimated after rescaling the hominin phylogeny to generations

using a constant generation time of 25 years (52). A generalized least squares approach

(53) implemented in the package 'Phylogenetics' for *Mathematica* (54) was used to

estimate a constant per-generation variance rate for each variable (log-size and PC

scores) based on available data.

Using trait-specific constant per generation rates, evolutionary change was simulated as

a uni- or multidimensional random walk (12) on the hominin phylogeny. Simulations

were run 1,000 times and the mean change between all ancestors and descendants was

used as the expectation of the amount of change if each branch had evolved neutrally

under a pure BM model. For endocranial and dental shape, this simulation was

performed in PC morphospace. Shape distances between ancestors and descendants

were calculated as the square root of the sum of the squared differences in all PC scores

between two given species, which is equivalent to the definition of Procrustes distance

for landmark data. For dental and endocranial size, branch-specific amounts of change

were calculated simply as the difference between descendants and ancestors.

Transformations between landmark coordinates and PC morphospace were done with

the package 'Geometric Morphometrics' for *Mathematica* (55).

422   The mvBM branch-specific changes were compared to the pure BM changes as the ratio

423   mvBM/BM. A value larger than 1 indicates that a given branch has experienced more

424   change than expected under a BM model (that is, that branch has evolved faster than

425   expected under a neutral model regardless of the directionality of the change). A value

426   smaller than 1 is indicative of slower evolution than that expected under a neutral

427   model, which is in turn indicative of stabilizing selection along a certain branch. As we

428   emphasized earlier, although we refer to these values as *rates*, we recognize that they

429   are not rates in the strict sense, but the ratio of observed to simulated change per branch.

430   These values were color coded and overlaid on the original phylogeny.

431

440

441   **References**

442

443   1.   Pilbeam D, Gould SJ (1974) Size and scaling in human evolution. *Science*

444   186(4167):892-901.

445   2.   McHenry HM (1982) The pattern of human evolution: Studies on bipedalism,

446   mastication, and encephalization. *Ann Rev Anthropol* 11:151-173.

447   3.   Jiménez-Arenas JM, Pérez-Claros JA, Aledo JC, Palmqvist P (2014) On the

448   relationships of postcanine tooth size with dietary quality and brain volume in

449   primates: Implications for hominin evolution. *BioMed Res Int* 2014:1-11.

450   4.   Aiello LC, Wheeler P (1995) The expensive-tissue hypothesis: The brain and the

451   digestive system in human and primate evolution. *Curr Anthropol* 36(2):199-

452   221.

453   5.   Ungar PS (2012) Dental evidence for the reconstruction of diet in African early

454   *Homo*. *Curr Anthropol* 53(S6):S318-S329.

455   6.   Spoor F, et al. (2015) Reconstructed *Homo habilis* type OH 7 suggests deep-

456   rooted species diversity in early *Homo*. *Nature* 519(7541):83-86.

457   7.   Arsuaga JL, et al. (2014) Neandertal roots: Cranial and chronological evidence

458   from Sima de los Huesos. *Science* 344(6190):1358-1363.

459   8.   Harmand S, et al. (2015) 3.3-million-year-old stone tools from Lomekwi 3, West

460   Turkana, Kenya. *Nature* 521(7552):310-315.

461   9.   Venditti C, Meade A, Pagel M (2011) Multiple routes to mammalian diversity.

462   *Nature* 479(7373):393-396.

463   10.   Smaers JB, Mongle CS, Kandler A (2016) A multiple variance Brownian motion

464   framework for estimating variable rates and inferring ancestral states. *Biol J*

465   *Linn Soc* 118(1):78-94.

466   11.   Wood B, K. Boyle E (2016) Hominin taxic diversity: Fact or fantasy? *Am J Phys*

467   *Anthropol* 159(S61):S37-S78.

468   12.   Polly PD (2004) On the simulation of the evolution of morphological shape:

469   Multivariate shape under selection and drift. *Palaeontologia Electronica* 7(2):1-

470   28.

471   13.   Holloway RL (1966) Cranial capacity, neural reorganization, and hominid

472   evolution: A search for more suitable parameters. *Am Anthropol* 68(1):103-121.

473   14.   Lieberman DE, McBratney BM, Krovitz G (2002) The evolution and

474   development of cranial form in *Homo sapiens*. *Proc Natl Acad Sci USA*

475   99(3):1134-1139.

476   15.   Bruner E, Manzi G, Arsuaga JL (2003) Encephalization and allometric

477   trajectories in the genus *Homo*: Evidence from the Neandertal and modern

478   lineages *Proc Natl Acad Sci USA* 100(26):1535-1540.

479   16.   Gunz P, Neubauer S, Maureille B, Hublin J-J (2010) Brain development after

480   birth differs between Neanderthals and modern humans. *Curr Biol* 20(21):R921-

481   R922.

482   17.   Bruner E, Iriki A (2016) Extending mind, visuospatial integration, and the

483   evolution of the parietal lobes in the human genus. *Quat Int* 405(Part A):98-110.

484   18.   Martínez-Abadías N, et al. (2012) Pervasive genetic integration directs the

485   evolution of human skull shape. *Evolution* 66(4):1010-1023.

486   19.   Stringer C (2016) The origin and evolution of *Homo sapiens*. *Phil Trans R Soc B*

487   *Biol Sci* 371(1698).

488   20.   Wolpoff MH (1971) *Metric Trends in Hominid Dental Evolution* (Press of Case

489   Western Reserve University, Cleveland).

490   21.   Organ C, Nunn CL, Machanda Z, Wrangham RW (2011) Phylogenetic rate

491   shifts in feeding time during the evolution of *Homo*. *Proc Natl Acad Sci USA*

492   108(35):14555-14559.

493   22.   Evans AR, et al. (2016) A simple rule governs the evolution and development of

494   hominin tooth size. *Nature* 530(7591):477-480.

495   23.   Gomez-Robles A (2016) Palaeoanthropology: What teeth tell us. *Nature*

496   530(7591):425-426.

497   24.   Wood B, Constantino P (2007) *Paranthropus boisei*: Fifty years of evidence and

498   analysis. *Am J Phys Anthropol* 134(S45):106-132.

499   25.   Bailey SE, Weaver TD, Hublin J-J (2009) Who made the Aurignacian and other

500   early Upper Paleolithic industries? *J Hum Evol* 57(1):11-26.

501   26.   Gómez-Robles A, Bermúdez de Castro JM, Arsuaga J-L, Carbonell E, Polly PD

502   (2013) No known hominin species matches the expected dental morphology of

503   the last common ancestor of Neanderthals and modern humans. *Proc Natl Acad*

504   *Sci USA* 110(45):18196-18201.

505   27.   Lande R (1976) Natural selection and random genetic drift in phenotypic

506   evolution. *Evolution* 30(2):314-334.

507   28.   Gómez-Robles A, Hopkins WD, Schapiro SJ, Sherwood CC (2015) Relaxed

508   genetic control of cortical organization in human brains compared with

509   chimpanzees. *Proc Natl Acad Sci USA* 112(48):14799-14804.

510   29.   Strait D, Grine FE, Fleagle JG (2015) Analyzing hominin phylogeny: Cladistic

511   approach. *Handbook of Paleoanthropology*, eds Henke W , Tattersall I (Springer

512   Berlin Heidelberg), pp 1989-2014.

513   30.   Dembo M, Matzke NJ, Mooers AØ, Collard M (2015) Bayesian analysis of a

514   morphological supermatrix sheds light on controversial fossil hominin

515   relationships. *Proc R Soc B Biol Sci* 282(1812).

516   31.   Rightmire GP (2004) Brain size and encephalization in early to Mid-Pleistocene

517   *Homo*. *Am J Phys Anthropol* 124(2):109-123.

518 32. Herculano-Houzel S (2009) The human brain in numbers: A linearly scaled-up

519   primate brain. *Front Hum Neurosci* 3:31.

520 33. Rosenberg KR (1992) The evolution of modern human childbirth. *Am J Phys*

521   *Anthropol* 35(S15):89-124.

522 34. Dunsworth HM, Warrener AG, Deacon T, Ellison PT, Pontzer H (2012)

523   Metabolic hypothesis for human altriciality. *Proc Natl Acad Sci USA*

524   109(38):15212-15216.

525 35. Ackermann RR, Cheverud JM (2004) Detecting genetic drift versus selection in

526   human evolution. *Proc Natl Acad Sci USA* 101(52):17946-17951.

527 36. Schroeder L, Roseman CC, Cheverud JM, Ackermann RR (2014)

528   Characterizing the evolutionary path(s) to early *Homo*. *PLoS ONE*

529   9(12):e114307.

530 37. Weaver TD, Roseman CC, Stringer CB (2007) Were Neandertal and modern

531   human cranial differences produced by natural selection or genetic drift? *J Hum*

532   *Evol* 53(2):135-145.

533 38. Meyer M, et al. (2016) Nuclear DNA sequences from the Middle Pleistocene

534   Sima de los Huesos hominins. *Nature* 531(7595):504-507.

535 39. Meyer M, et al. (2014) A mitochondrial genome sequence of a hominin from

536   Sima de los Huesos. *Nature* 505:403-406.

537 40. Gómez-Robles A, Polly PD (2012) Morphological integration in the hominin

538   dentition: evolutionary, developmental, and functional factors. *Evolution*

539   66(4):1024-1043.

540 41. Holloway RL, Broadfield DC, Yuan MS (2004) *The Human Fossil Record,*

541   *Brain Endocasts: The Paleoneurological Evidence* (Wiley-Liss, New York).

542   42.   Rohlf FJ, Slice D (1990) Extension of the Procrustes method for the optimal

543   superimposition of landmarks. *Syst Zool* 39(1):40-59.

544   43.   Bruner E, Grimaud-Hervé D, Wu X, de la Cuétara JM, Holloway R (2015) A

545   paleoneurological survey of *Homo erectus* endocranial metrics. *Quat Int* 368:80-

546   87.

547   44.   Wood B, Collard M (1999) The human genus. *Science* 284(5411):65-71.

548   45.   Strait DS, Grine FE (2004) Inferring hominoid and early hominid phylogeny

549   using craniodental characters: The role of fossil taxa. *J Hum Evol* 47(6):399-

550   452.

551   46.   Kluge AG (1989) A concern for evidence and a phylogenetic hypothesis of

552   relationships among Epicrates (Boidae, Serpentes). *Syst Biol* 38(1):7-25.

553   47.   Kimbel WH, et al. (2006) Was *Australopithecus anamensis* ancestral to *A.*

554   *afarensis*? A case of anagenesis in the hominin fossil record. *J Hum Evol*

555   51(2):134-152.

556   48.   Villmoare B, et al. (2015) Early *Homo* at 2.8 Ma from Ledi-Geraru, Afar,

557   Ethiopia. *Science* 347(6228):1352-1355.

558   49.   Gómez-Robles A, Bermúdez de Castro JM, Martinón-Torres M, Prado-Simón L,

559   Arsuaga JL (2015) A geometric morphometric analysis of hominin lower

560   molars: Evolutionary implications and overview of postcanine dental variation. *J*

561   *Hum Evol* 82:34-50.

562   50.   Pagel M (2002) Modelling the evolution of continuously varying characters on

563   phylogenetic trees: The case of hominid cranial capacity. *Morphology, Shape*

564   *and Phylogeny*, eds MacLeod N , Forey PL (Taylor & Francis, London), pp

565   269–286.

566   51.   Smaers JB (2014) evomap: R package for the evolutionary mapping of

567   continuous traits (Github: https://github.com/JeroenSmaers/evomap).

568   52.   Weaver TD, Roseman CC, Stringer CB (2008) Close correspondence between

569   quantitative- and molecular-genetic divergence times for Neandertals and

570   modern humans. *Proc Natl Acad Sci USA* 105(12):4645-4649.

571   53.   Martins EP, Hansen TF (1997) Phylogenies and the comparative method: A

572   general approach to incorporating phylogenetic information into the analysis of

573   interspecific data. *Am Nat* 149(4):646-667.

574   54.   Polly PD (2014) Phylogenetics for Mathematica. Version 3.0 (Department of

575   Geological Sciences, Indiana University, Bloomington, Indiana).

576   55.   Polly PD (2016) Geometric Morphometrics for Mathematica. Version 12.0

577   (Department of Geological Sciences, Indiana University, Bloomington, Indiana).

578

579

580
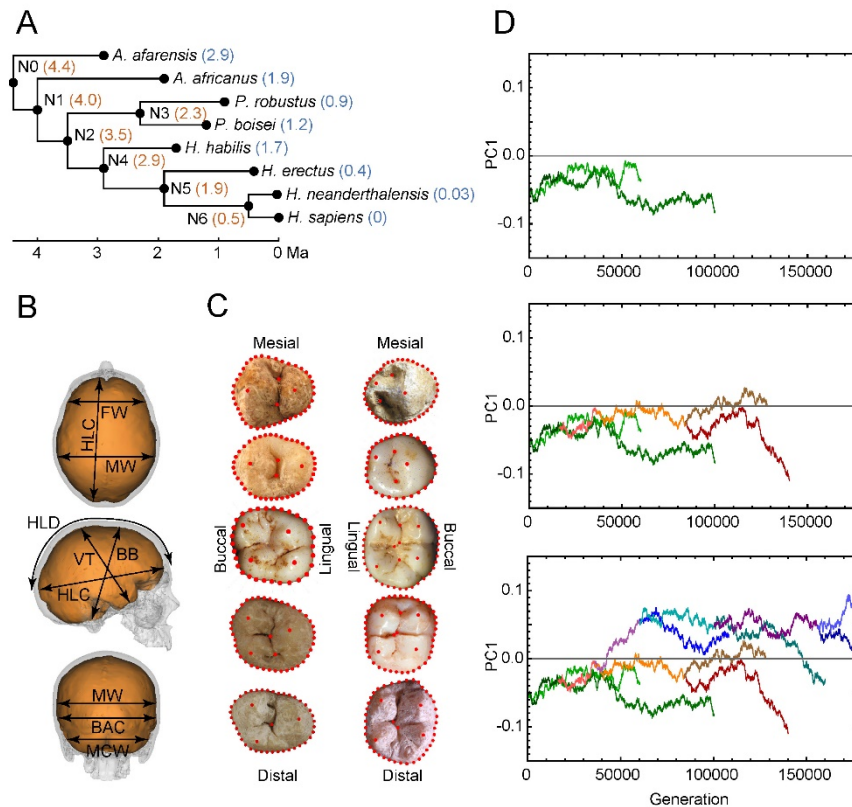
Fig. 1. Methodological setup of the study. (*A*) Hominin phylogeny employed in our

analyses, indicating the dates used for terminal species (blue) and nodes (orange). (*B*)

Linear metrics used in the study of endocranial variation. FW: frontal width at Broca's

cap; HLC: hemispheric length chord; MW: maximum endocranial width; HLD:

hemispheric length dorsal arch; BB: basion-bregma distance; VT: vertex-lowest

temporal distance; BAC: biasterionic chord; MCW: maximum cerebellar width. (*C*)

Landmark and semilandmark datasets used in the study of postcanine dental variation.

Upper teeth are on the left and lower teeth on the right. Postcanine teeth are represented

from top to bottom following the sequence P3, P4, M1, M2 and M3. (*D*) Brownian

motion simulation of the evolution of one trait (PC1 score) across the hominin

phylogeny. Top: green shading shows evolution along the *A. afarensis* and *A. africanus*

branches. Middle: simulated evolution along the *Paranthropus* clade is added in orange-

red shading to the above plot. Bottom: simulated evolution along the *Homo* clade is

594   added as blue shading to the above graph. B and C have been modified after refs. (26,

595   43).

596

597
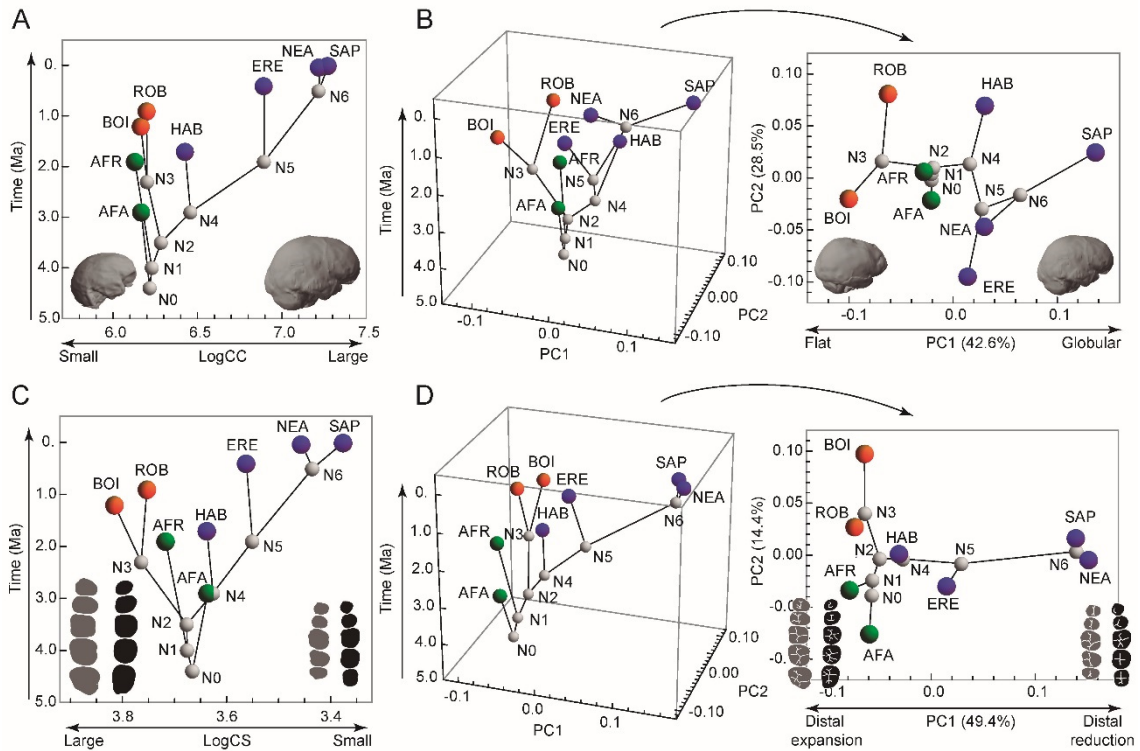
Fig. 2. Variation in endocranial and dental size and shape through time. (*A*) Change in endocranial size (logarithm of cranial capacity) over time showing extreme examples of variation. (*B*) Principal components analysis of endocranial shape variation over time is shown on the left, and the projection of PC1 and PC2 without time is represented on the right. (*C*) Change in dental size (logarithm of centroid size) over time. (*D*) Principal components analysis of dental shape variation over time (left), and without time (right). In *A* and *B*, the small and flat endocasts are the *A. afarensis* Sts 5 and *P. robustus* SK 1585 specimens. The large and globular endocast is a recent *H. sapiens*. Endocasts are in the same orientation as in Figure 1. In *C* and *D* dental silhouettes representing large and distally expanded dentitions are based on the *P. robustus* specimens SK 13/14 (upper teeth) and SK 23 (lower teeth). Small and distally reduced dentitions are based on a recent *H. sapiens*. Orientation of teeth is the same as

611   in Figure 1. AFA: *A. afarensis*; AFR: *A. africanus*; ROB: *P. robustus*; BOI: *P. boisei*;

612   HAB: *H. habilis*; ERE: *H. erectus*; NEA; *H. neanderthalensis*; SAP: *H. sapiens*.

613
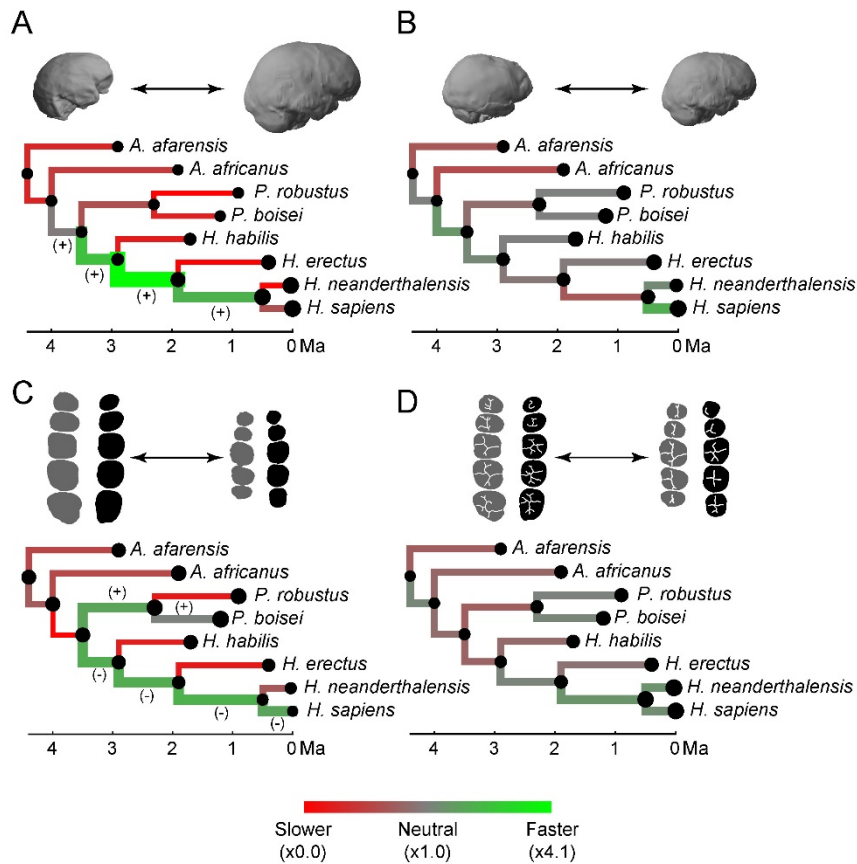
Fig. 3. Evolution of endocranial and dental size and shape. (*A*) Comparison of

observed and simulated branch-specific amounts of endocranial size variation. (*B*)

Comparison of observed and simulated amounts of endocranial shape variation. (*C*)

Comparison of observed and simulated amounts of dental size variation. (*D*)

Comparison of observed and simulated amounts of dental shape variation. Red

represents stasis along a given branch and green represents fast evolution along a given

branch, regardless of the directionality of change. Branch thickness is proportional to

the observed amount of change along a given branch. In *A* and *C*, (+) represents size

increase and (–) represents size decrease along fast-evolving branches, and tip and node

size is proportional to endocranial and dental size. In *B* and *D* the amount of change per

branch is based on shape distances that include all dimensions of the morphospace, and

node and tip size is proportional to the amount of shape change with respect to the

627   ancestral-most node. Example specimens are the same as in Figure 2. Orientation of

628   endocasts and teeth is the same as in Figures 1 and 2.

629